Intrinsically Switchable Thin Film Ferroelectric Resonators

Seyit Ahmet Sis, Victor Lee, Jamie D. Phillips and Amir Mortazawi

Department of Electrical Engineering and Computer Science, University of Michigan,
Ann Arbor, MI 48109, USA

***Abstract* — This paper presents DC voltage dependent thin film bulk acoustic wave resonators (FBARs) based on ferroelectric barium strontium titanate (BST). The electrostrictive effect in BST film that enables the resonances to switch on and off with dc bias is discussed. Composite BST FBARs that consist of BST, platinum (Pt), silicon (Si), and oxide (SiO_2) layers are discussed by comparing with the conventional FBAR structure. For composite FBARs, the BST layer is primarily used for transduction while the Si and SiO_2 layers are used to increase the overall quality factor (*Q*). Measurement results of a composite FBAR show a *Q* that exceeds 600 at its parallel resonance frequency of 2.169 GHz and an electromechanical coupling coefficient of 0.68%.**

***Index Terms* — Barium strontium titanate, ferroelectric devices, thin film bulk acoustic wave resonators (FBAR), composite FBAR, intrinsically switchable devices**

I. Introduction

Ferroelectric materials such as BST, barium titanate (BTO) and strontium titanate (STO) have a strong electrostrictive effect [1]. Electrostriction is an attractive property because it can be represented as an electric field dependent piezoelectric effect. When a dc bias is applied to ferroelectrics, they act as a piezoelectric and can be used to design resonators that intrinsically switch on and off. Due to this property, many groups have been working on BST and BTO based FBARs [2], lateral mode resonators [3]-[4], and solidly mounted resonators (SMR) [5]-[6]. Recently, a composite BST FBAR with additional Si/SiO_2 layers has been presented to improve quality factors [7] by applying the method in [8] to BST based materials.

In this paper, the general properties of intrinsically switchable thin film ferroelectric resonators based on BST are presented. Electrostriction in BST films and the structure of both conventional and composite BST FBARs are discussed. The acoustic transmission line model that is used in designing the composite FBARs is explained. The measurement results of a composite FBAR resonator and corresponding Modified Butterworth-Van Dyke (MBVD) model are presented. A composite BST FBAR has been measured with a quality factor as high as 617 at 2.169 GHz.

II. Electrostriction In BST

A one dimensional electrostriction equation can be used to relate mechanical strain to applied electric field [9].

$$u = QP^2 \tag{1}$$

$$P = P_s + \chi E \tag{2}$$

In (1), *u, Q,* and *P* are the strain, electrostriction coefficient, and electric polarization, respectively. *P* is the summation of the spontaneous (P_s) and electric field induced polarization as shown in (2). By substituting (2) into (1), strain as a function of the electric field can be derived as follows,

$$u = QP_s^2 + 2QP_s\chi E + Q\chi^2 E^2. \tag{3}$$

In the right hand side of (3), the first, second, and third terms correspond to strains due to spontaneous polarization, piezoelectricity, and electrostriction, respectively [9]. Equation (3) can be expressed as follows,

$$u = QP_s^2 + (2QP_s\chi + Q\chi^2 E)E. \tag{4}$$

In (4), the two terms in the parenthesis can be thought of as the effective piezoelectric coefficient since *u* and *E* are linearly dependent with respect to one another. While the first term of the effective piezoelectric coefficient is constant, the second term is *E* field dependent. Therefore, electrostriction can be considered as *E* field dependent piezoelectricity [10]. Since BST is in the paraelectric phase at room temperature, the spontaneous polarization is not present (P_s=0) and (4) can be simplified as follows,

$$u = (Q\chi^2 E)E. \tag{5}$$

As it is seen in (5), electromechanical transduction occurs primarily through the electrostrictive effect in BST.

III. Conventional and Composite FBAR Structures

The cross-section of a conventional and composite FBAR is shown in Fig. 1. In composite FBARs, Si and SiO_2 layers are used to increase the overall quality factor and mechanical strength. The disadvantage of composite FBARs is its reduced effective electromechanical coupling coefficient (K_t^2). However, it can be maximized for the desired resonance mode by properly choosing the thickness of each layer [8].

In addition, conventional FBARs, as opposed to composite FBARs, do not exhibit even order resonance modes since there is no electromechanical transduction at even order modes due to symmetric mechanical displacement across the BST layer [8].

978-1-4673-1088-8/12/$31.00 ©2012 IEEE

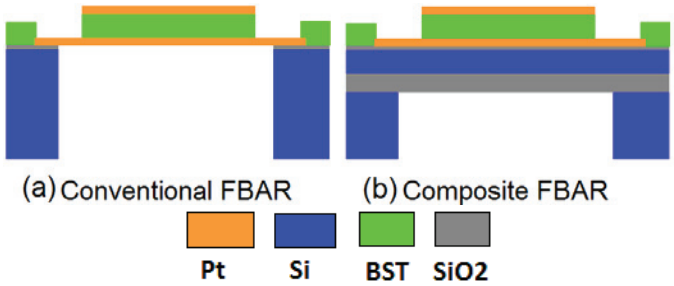

Fig. 1. (a) Conventional and (b) composite FBAR structures.

IV. Acoustic Transmission Line Model of Composite FBARs

The acoustic transmission line (TL) model, as seen in Fig. 2 can be utilized in the design and analysis of composite FBARs [11]. Each layer in the composite structure can be modeled as an acoustic transmission line. The impedance of the air is transferred to acoustic impedances of Z_t and Z_b, as seen in Fig. 2, through the successive layers by using

$$Z = Z_{ac}\frac{Z_L + Z_{ac}\tanh(\gamma t)}{Z_{ac} + Z_L\tanh(\gamma t)} \tag{6}$$

where γ, t, Z_{ac}, and Z_L are the acoustic propagation constant, thickness of each layer, acoustic impedance of each layer, and acoustic impedance seen looking into previous layer, respectively. Once Z_t and Z_b are determined, they are substituted into (7) to obtain electrical input impedance Z_{in}.

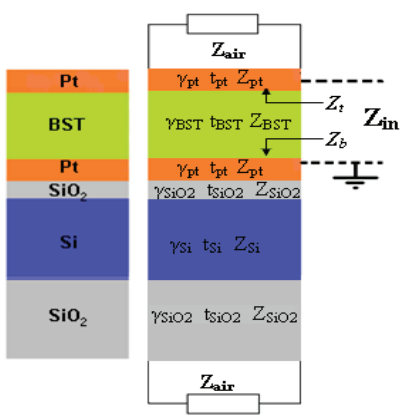

Fig. 2. Acoustic TL model for composite FBARs.

$$Z_{in} = \frac{1}{j\omega C}\times\left[1 - K^2\frac{\tan\varphi}{\varphi}\frac{(z_t+z_b)\cos^2\varphi + j\sin 2\varphi}{(z_t+z_b)\cos 2\varphi + j(z_t z_b+1)\sin 2\varphi}\right] \tag{7}$$

where C is static capacitance, K^2 is the electromechanical coupling coefficient of BST, and φ is half of the acoustic phase delay in the BST layer [11].

VI. Fabrication of Composite FBARs

Composite FBARs are fabricated on a 400 µm thick silicon-on-insulator (SOI) wafer. The SOI wafer has 2.5 µm of high resistivity device Si and a 2 µm layer of buried SiO_2. A 100 nm layer of thermal SiO_2 is grown on top of the device Si. A 100 nm layer of platinum is then deposited and patterned to serve as the bottom electrode. A 300 nm layer of BST layer is deposited by pulsed laser deposition (PLD) with a substrate temperature of 650 °C and in a 300 mT oxygen environment. Afterwards, a 100 nm layer of platinum is deposited and patterned to serve as the bottom electrode. The BST thin film is then selectively etched using diluted HF to reach the bottom electrode of the device. A 500 nm layer of gold is then deposited to serve as the probe contact pads. Finally, the thick Si handling layer underneath of the device is etched through deep reactive ion etching (DRIE).

VI. Measurement Results

The fabricated resonator is measured with 150 µm pitch size GSG probes. *S*-parameters are acquired by using an Agilent E8364B vector network analyzer. The resonator is biased through the measurement port by using a bias tee. The microscope photo of the measured device is shown in Fig. 3.

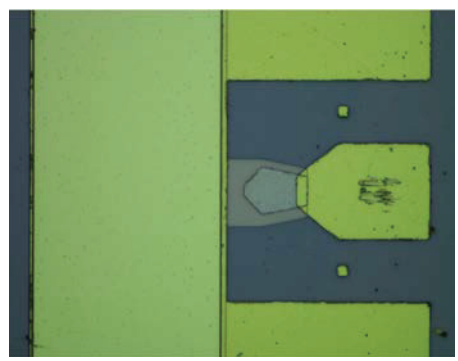
Fig. 3. Microscope photo of the measured device.

The quality factor of the resonator is calculated by the phase of input impedance using

$$Q = \frac{f}{2}\left|\frac{d\phi_{Zin}}{df}\right|. \tag{8}$$

The K_t^2 is calculated based on the measured results by using

$$K_t^2 = \frac{\pi}{2}\frac{f_s}{f_p}\tan\left(\frac{\pi}{2}\frac{(f_p - f_s)}{f_p}\right) \tag{9}$$

where f_s and f_p denote the series and parallel resonance frequencies, respectively.

The input impedance of the resonator is shown in Fig. 4. When the device is biased at 16 V and is switched on, 9 resonance modes are seen in the frequency range of 500 MHz to 6.5 GHz. Maximum Q for the resonator is achieved at the 3rd resonance mode and has Qs of 448 and 617 with f_s and f_p of 2.163 GHz and 2.169 GHz, respectively. Maximum K_t^2 of 3.3% for the resonator is achieved at the 5th resonance mode, f_s and f_p of which are 3.360 GHz and 3.408 GHz, respectively.

978-1-4673-1088-8/12/$31.00 ©2012 IEEE

When there is no DC bias applied, the resonances are off and act as a capacitor.

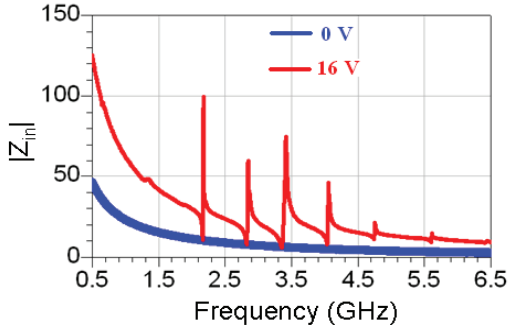

Fig. 4. Input impedance of measured resonator at 0 V and 16 V bias voltages.

The MBVD model is fitted to the measurement results of the composite FBAR for the 3rd resonance mode at 16 V DC bias. The schematic of the MBVD model and fitting results are given in Fig. 5. The fitted MBVD model component values are shown in Table I.

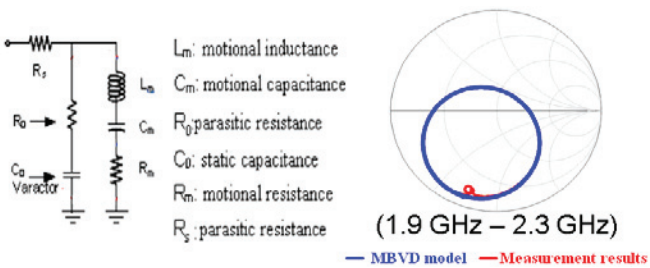

Fig. 5. Modified Butterworth-Van Dyke Model.

TABLE I
MBVD MODEL PARAMETERS FOR THE MEASURED COMPOSITE FBAR

	C_0 (pF)	Cm (fF)	Lm (nH)	Rm (Ohm)	Rs (Ohm)	R_0 (Ohm)
Value	2.34	14.65	369.7	9.1	2.8	0.7

VII. Conclusion

In this paper, electrostrictive effect in BST films is discussed and the conventional and composite FBARs are compared. By utilizing the electrostrictive property of BST and low acoustic loss of Si and SiO_2, an intrinsically switchable composite FBAR resonator with a quality factor as high as 617 is obtained. Effort in further increasing the Q of intrinsically switchable thin film ferroelectric resonators by optimizing BST deposition parameters is currently ongoing.

Acknowledgment

This work is partially funded by the National Science Foundation and ARL MAST program. It is performed at the Lurie Nanofabrication Facility, a member of the National Nanotechnology Infrastructure Network, which is supported in part by the National Science Foundation.

References

[1] S. Gevorgian, *Ferroelectrics in Microwave Devices, Circuits and Systems: Physics, Modeling, Fabrication and Measurements*. New York: Springer-Verlag, 2009.

[2] Xinen Zhu; Phillips, J.D.; Mortazawi, A.; , "A DC Voltage Dependant Switchable Thin Film Bulk Wave Acoustic Resonator Using Ferroelectric Thin Film," *Microwave Symposium, 2007. IEEE/MTT-S International* , vol., no., pp.671-674, 3-8 June 2007

[3] Xinen Zhu; Lee, V.; Phillips, J.; Mortazawi, A.; , "Intrinsically switchable contour mode acoustic wave resonators based on barium titanate thin films," *Microwave Symposium Digest, 2009. MTT '09. IEEE MTT-S International* , vol., no., pp.93-96, 7-12 June 2009

[4] Lee, V. C.; Sis, S. A.; Zhu, X.; Mortazawi, A.; , "Intrinsically switchable interdigitated barium titanate thin film contour mode resonators," *Microwave Symposium Digest (MTT), 2010 IEEE MTT-S International* , vol., no., pp.1-1, 23-28 May 2010

[5] Vorobiev, A.; Gevorgian, S.; , "Tunable BaxSr1−xTiO3 FBARs based on SiO2/W Bragg reflectors," *Microwave Symposium Digest (MTT), 2010 IEEE MTT-S International* , vol., no., pp.1444-1447, 23-28 May 2010

[6] Saddik, George N.; Boesch, Damien S.; Stemmer, Susanne; York, Robert A.; , "Strontium titanate DC electric field switchable and tunable bulk acoustic wave solidly mounted resonator," *Microwave Symposium Digest, 2008 IEEE MTT-S International* , vol., no., pp.1263-1266, 15-20 June 2008

[7] Sis, S.A.; Lee, V.; Mortazawi, A.; , "Intrinsically switchable, BST-on-silicon composite FBARs," *Microwave Symposium Digest (MTT), 2011 IEEE MTT-S International* , vol., no., pp.1-4, 5-10 June 2011

[8] Lakin, K. M.; Wang, J. S.; , "Acoustic bulk wave composite resonators," Applied Physics Letters , vol.38, no.3, pp.125-127, Feb 1981

[9] D.-Y. Chen and J. Phillips, "Electric field dependence of piezoelectric coefficient in ferroelectric thin films," *J. Electroceram.,* no. 17, pp. 613-617, 2006.

[10] D. Damjanovic and R.E. Newnham, "Electrostrictive and piezoelectric materials for actuator applications," *J.of Intell. Mater. Syst. and Struct.,* vol.3, pp. 190-208, Apr. 1992.

[11] Lakin, K.M.; Kline, G.R.; McCarron, K.T.; , "High-Q microwave acoustic resonators and filters," *Microwave Theory and Techniques, IEEE Transactions on* , vol.41, no.12, pp.2139-2146, Dec 1993